Microelectronic Engineering 150 (2016) 26–31

Contents lists available at ScienceDirect

Microelectronic Engineering

journal homepage: www.elsevier.com/locate/mee

# Al-doped ZnO thin films deposited by confocal sputtering as electrodes in ZnO-based thin-film transistors

N. Hernandez-Como [a,*], A. Morales-Acevedo [b], M. Aleman [a], I. Mejia [c], M.A. Quevedo-Lopez [c]

[a] Centro de Nanociencias y Micro y Nanotecnologías, Instituto Politécnico Nacional, México, Mexico
[b] Departamento de Ingeniería Eléctrica, Centro de Investigación y de Estudios Avanzados del Instituto Politécnico Nacional, México, D.F., Mexico
[c] Department of Materials Science and Engineering, University of Texas at Dallas, USA

ARTICLE INFO

*Article history:*
Received 26 August 2015
Received in revised form 26 October 2015
Accepted 28 October 2015
Available online 30 October 2015

*Keywords:*
Al-doped zinc oxide
Thin film transistors
RF sputtering
Specific contact resistance

ABSTRACT

Aluminum doped zinc oxide (AZO) films were deposited by confocal RF magnetron sputtering at different substrate temperatures. AZO films with a transparency up to 90% in the visible spectrum were obtained. Polycrystalline AZO films, with planes in the (002) and (103) orientations of the zincblende (hexagonal) structure, were obtained at substrate temperatures higher than 60 °C. The best AZO films, obtained at 75 °C, showed an electrical resistivity of $8.8 \times 10^{-4}$ Ω-cm, with a carrier concentration of $4 \times 10^{20}$ $cm^{-3}$ and mobility of 20 $cm^2$/V-s. These are appropriate values for solar cell applications. In addition, ZnO-based thin-film transistors (TFTs) were fabricated for evaluating the behavior of the AZO films as source and drain contacts on the transistors. The field effect mobility and the threshold voltage of the fabricated devices were 20 $cm^2$/V-s and 7 V, respectively. The TFTs showed an $I_{on}/I_{off}$ ratio of up to 9 orders of magnitude. A specific contact resistance of approximately 0.06 Ω-$cm^2$ was determined for the AZO/ZnO interface. This result corresponds to the first report of the ZnO/AZO specific contact resistance obtained with a maximum processing temperature of 100 °C. Therefore, this TFT technology is fully compatible with flexible substrates and can be used for transparent and large area electronics.



## 1. Introduction

Electrical and optical properties of zinc oxide (ZnO) thin films can be manipulated by extrinsic doping with Ga, Al, In, B, F, Si, Ge, Y, Sc, Ti, Hf and Zr [1]. Aluminum and gallium doped ZnO films have demonstrated high transparency above 90% in the visible spectrum, as well as low electrical resistivity in the range of $10^{-4}$ Ω-cm. Aluminum-doped zinc oxide (AZO) is a potential candidate material to be used as a transparent conductive oxide (TCO) as an alternative of indium tin oxide (ITO). Some advantages of AZO over ITO and others TCOs are the low cost of manufacture, abundant raw material, high temperature stability and non-toxicity against a shortage of indium in the future and an increment in its price per kilogram [2]. AZO films are mainly used as transparent electrodes for organic and inorganic light emitting diodes (LEDs), thin-film transistors (TFTs) and thin-film solar cells [3–6].

On the other hand, RF magnetron sputtering is a popular method to deposit both ZnO and AZO films. It is widely used to obtain uniform films with high packing densities and high deposition rates. The electrical and optical properties of AZO films obtained with this deposition method are highly dependent on the sputtering conditions such as RF power, gas flow, pressure, and substrate temperature [7,8]. The aluminum content in the sputtering target and film post-deposition treatments, like annealing and chemical etching, also affect the electrical and optical properties of the AZO films [9].

Previous works for AZO deposition have demonstrated that optical (transmittance > 85%) and electrical (resistivity < $3 \times 10^{-4}$ Ω-cm) properties can be controlled by varying the deposition pressure, the RF power and the substrate temperature [10–13]. A key in these reports is to have very thick films (>700 nm) to improve film crystallinity and sheet resistance. Most of this work has been done using target to substrate distances of around 5–10 cm. These distances are used for direct sputtering (substrate parallel to the target) which has the inconvenience that only one material can be sputtered at a time. Also, the target must be larger than the substrate to yield acceptable film uniformity.

However, only few reports have been made on optimizing AZO films obtained by confocal sputtering [14,15], where the target is positioned at an angle relative to the substrate surface allowing the deposition of multiple materials in series or co-deposited without breaking the vacuum. In confocal sputtering, the target size is necessarily smaller than the substrate. So far, the AZO properties obtained by confocal sputtering have always been inferior to the ones deposited by direct sputtering. The motivation of this work is to use confocal deposition of AZO films with the possibility to fabricate ZnO-based TFTs in one single chamber, such as our group has demonstrated by pulsed laser deposition (PLD)

* Corresponding author.
*E-mail address:* nohernandezc@ipn.mx (N. Hernandez-Como).

http://dx.doi.org/10.1016/j.mee.2015.10.017
0167-9317/

[16]. This demonstrates the potential use of confocal sputtering for the development of optimized AZO films with improved usage of the target and substrate size for large area applications.

In this work, we explore the impact of the substrate temperature in both electrical and optical properties of AZO thin films deposited using confocal sputtering. Then, the best AZO films were evaluated as source and drain electrodes in ZnO-based TFTs as a potential alternative to ITO contacts. The TFTs performance was uniform over a 4 in. wafer while the AZO and ZnO target sizes were 2 in. each.

## 2. Experimental details

AZO thin films were deposited both on glass and on (100) CZ n-type crystalline silicon 1 in. square substrates. Prior to deposition, each substrate was cleaned in acetone, isopropanol, deionized sonicated water and dried in nitrogen. An ATC Orion RF magnetron sputtering system, made by AJA International, with a base pressure of $2.7 \times 10^{-6}$ Pa was used. The 2 in. diameter target material was a mixture of ZnO (99.999% purity) and aluminum oxide ($Al_2O_3$) (99.99% purity), with a 98/2 wt.% content of ZnO/$Al_2O_3$ from Kurt J. Lesker Company. The distance between the sputtered target and the substrate was fixed to 25 cm. The confocal angle was fixed to 30° and the substrate was rotated during all the deposition time. For all the depositions, a constant flow of 20 sccm of argon was used. From preliminary work, at room temperature, it was found that the deposition rate increased linearly with the increase of the RF power from 50 to 300 W. In order to avoid permanent damage in the AZO target due to overheating and for maintaining a reasonable deposition rate (4 nm/min), the RF power was fixed to 100 W. The deposition pressure was selected to be 0.27 Pa (0.53 and 1.07 Pa were also studied) because at that pressure the refractive index, the bandgap, the average transmittance (in the visible spectrum 400–800 nm) and the resistivity of the AZO film were optimized to 1.9, 3.5 eV, 80% and $1.5 \times 10^{-3}$ Ω-cm, respectively. At higher deposition pressures, the films behaved more like undoped ZnO with resistivities higher than $10^{-1}$ Ω-cm and low dense films with refractive indexes around 1.7–1.8 were obtained. In order to achieve a transmittance higher than 90% and electrical resistivity in the order of $10^{-4}$ Ω-cm, the AZO films were deposited at different substrate temperatures from 20 to 100 °C.

Electrical resistivity, carrier concentration, carrier type and carrier mobility were measured by the Hall Effect technique. For Hall measurements, 1 $cm^2$ samples with indium contacts were used. The film on glass transmittance was obtained from a Shimadzu UV–2401PC UV–Vis spectrophotometer. The bandgap was calculated by plotting $\alpha^2$ versus $h\nu$ (photon energy) and extrapolating the linear portion of the plot to the $h\nu$ axis, as described elsewhere for direct bandgap semiconductors [17]. Structural analysis was made with a Rigaku Ultima III X-ray diffractometer (XRD), which uses a Cu Kα radiation (λ = 0.15406 nm), with $\theta$–$2\theta$ scans. The surface roughness and morphology were analyzed with a Veeco Dimension 5000 SPM atomic force microscope (AFM). Film thickness and refractive index were determined using a Sentech 800 spectroscopic ellipsometer.

ZnO-based TFTs were fabricated using photolithography processes developed by our group [16]. Here, a 30 nm thick ZnO film was deposited by RF sputtering, on top of the 90 nm $HfO_2$ gate dielectric, at room temperature, with a power of 100 W, pressure of 0.53 Pa and an Ar flow of 12 sccm. $HfO_2$ was deposited by atomic layer deposition at a temperature of 100 °C. Then, 500 nm of Parylene-C were deposited at room temperature to serve as the interlayer dielectric and as a hard mask for subsequent etching steps. After opening the source–drain vias, AZO was deposited to form source–drain (S–D) contacts. The dimensions of the devices were as follows: channel width $W = 80$ μm and channel length $L = 20$, 40 and 80 μm. The devices were characterized using a Keithley 4200 semiconductor characterization system under regular ambient and dark conditions.

## 3. Results and discussion

### 3.1. Material characterization

The estimated AZO deposition rate was 4 nm/min using both room temperature and RF power of 100 W. The same deposition time (25 min) was used for the different deposition temperatures producing a film thickness around 100 nm for all the films.

XRD analysis was used to obtain information about structural changes in the AZO films. XRD spectra for the different AZO films and the ZnO powder reference are shown in Fig. 1. No $Al_2O_3$ phase was found in the films. Several peaks were observed for the AZO films deposited at temperatures lower than 50 °C. In order to determine the preferential orientation in the AZO films at different substrate temperatures, the texture coefficient ($TC$) for each film was calculated according to [18]:

$$TC(hkl) = \frac{I(hkl)/I_0(hkl)}{N^{-1}\sum_N I(hkl)/I_0(hkl)} \quad (1)$$

where, $I(hkl)$ is the relative intensity of the peak at ($hkl$) direction, $I_0(hkl)$ is the relative intensity of the peak at ($hkl$) direction from the ZnO powder reference (036–1451), and $N$ is the number of observed reflections. The (002) crystallites had $3 < TC < 6$ in the temperature range from 20 to 60 °C and $1 < TC < 2$ in the temperature range from 75 to 100 °C. On the other hand, the (103) oriented crystallites had a $TC$ very close to 1 for temperatures below 50 °C, and above 50 °C the $TC$ became slightly greater than 1. The $TC$ for all the other ($hkl$) planes was lower than 1 for all the temperature range. This indicates that below 60 °C the crystallites are preferentially oriented along the (002) plane, but above 75 °C the film becomes more polycrystalline due to the increased contribution of the crystallites with the (103) orientation. The lattice parameters ($a$ and $c$), the grain size and the substrate temperature are shown in Table 1. It can be observed that the lattice parameter $c$ is greater than the corresponding bulk value. On the other

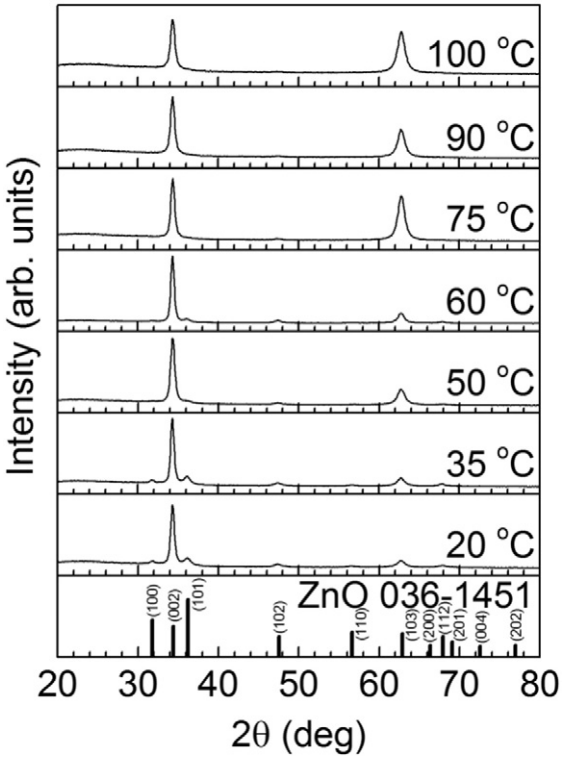


**Fig. 1.** XRD spectra of the AZO films deposited at different substrate temperatures.

**Table 1**
Lattice parameters and grain sizes for different substrate temperatures.

| Sample | Lattice parameter (Å) | | c/a | Grain size (nm) | |
|---|---|---|---|---|---|
| | c | a | | (002) | (103) |
| Powder reference | 5.20661 | 3.24982 | 1.60212 | – | – |
| 20 | 5.2242 | 3.2435 | 1.61064 | 16.8 | 10.2 |
| 35 | 5.2226 | 3.2436 | 1.61011 | 17.4 | 10.2 |
| 50 | 5.2213 | 3.2479 | 1.60756 | 15.2 | 9.7 |
| 60 | 5.2194 | 3.2457 | 1.60809 | 17.7 | 11.2 |
| 75 | 5.2156 | 3.2485 | 1.60551 | 16.0 | 10.2 |
| 90 | 5.2190 | 3.2453 | 1.60817 | 15.1 | 10.2 |
| 100 | 5.2168 | 3.2486 | 1.60585 | 14.9 | 9.3 |

hand the lattice parameter *a* is slightly lower than the bulk value. As the substrate temperature increases, the lattice parameter *c* tends to reduce to the bulk value, but the lattice parameter (***a***) remains almost constant. An increment in the substrate temperature improves the lattice parameter *c* due to the larger diffusion of the sputtering species, but at the expense of promoting polycrystalline films. At low substrate temperatures, the increment of the c lattice parameter has been associated to the bombardment of the sputtering species and the mismatch between the amorphous glass and ZnO [19]. A reduced lattice parameter is associated with the increased concentration of Al in AZO films [20], which is not the present case. The lattice parameter ratio *c*/*a*, also shown in Table 1, turned out to be 0.2–0.7% greater than the powder reference, with the best match at the substrate temperature of 75 °C. These results show that there is negligible strain in the AZO films due to the substrate. Crystallite domain sizes, evaluated with the Scherrer formula [18] as the substrate temperature increased from 20 to 100 °C, were in the range of 17.7 down to 14.9 nm and 11.2 down to 9.3 nm, for the (002) and (103) diffraction peaks, respectively. These results are shown in Table 1. As we will show later, the optical and electrical properties are not strongly affected by this size variation. At 60 °C both (002) and (103) oriented crystallite domains had the maximum size of 17.7 and 11.2 nm, respectively. In the literature, two cases were found where the AZO films showed dominant (103) peaks. In the first case, direct current magnetron sputtering was used, and according to the authors, the change in the preferred orientation was because of re-sputtering of the films by high-energy neutral oxygen atoms [21]. In the second case, direct current pulse reactive magnetron sputtering was used, and the authors associated the transition of the film growth from the (002) vertical growth to the (103) oriented lateral growth, to the evolution of the crystal face energy for long deposition times (3 h) [22]. In both cases, an ambient of argon/oxygen and a substrate temperature higher than 200 °C were used. In the present study, temperatures higher than 100 °C were not explored and all depositions were carried out without oxygen.

In Fig. 2, three-dimensional (3D) AFM images (1 μm × 1 μm) of the AZO films deposited at 20, 50, 75 and 100 °C are shown. The root mean squared (RMS) roughness for the AZO films was below 1.05 nm, which was the value for the AZO films deposited at a substrate temperature of 20 °C. For substrate temperatures higher than 50 °C, the AZO RMS roughness reached values down to 0.56 nm. This roughness reduction is related to the grain sizes reduction as estimated from XRD. Smooth and flat surfaces, like the ones obtained in this work, are necessary to fabricate high quality devices because they facilitate a homogeneous interface formation between different materials. As we will show later, the AZO films were used as top electrodes in ZnO-based TFTs, but further applications will require using them as bottom electrode like in organic TFTs [23].

The UV–Vis transmittance and the corresponding bandgap versus the substrate temperature are plotted in Fig. 3. The optical properties (transmittance) of the AZO films are improved with the increase of the substrate temperature. We can observe that there is a clear increase of the transmittance when the substrate temperature is higher than 60 °C. Below 60 °C, the average transmittance is below 75%, and above 60 °C it is around 90%. This result is related to the increased bandgap when the substrate temperature is higher than 60 °C. At 75, 90 and 100 °C, the average transmittance is above 90% and the bandgap is higher than 3.55 eV. The refractive index ($n$) at 633 nm turned out to be 1.9 for the complete set of AZO samples. This value is very close to that of the bulk crystalline ZnO ($n = 2$) which means that the obtained AZO films are dense and packed. It can be concluded that polycrystalline films promote transparent films. The increase in the transmittance when the deposition temperature is higher than 75 °C is related to the crystal structure change observed by XRD.

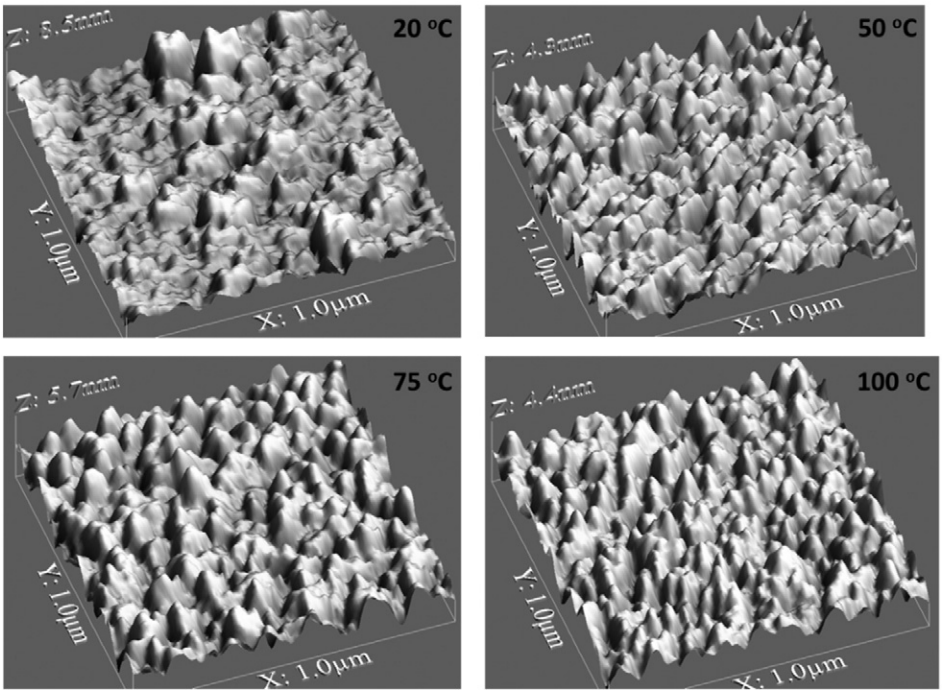


**Fig. 2.** AFM 3D images for the films deposited at 20, 50, 75 and 100 °C.

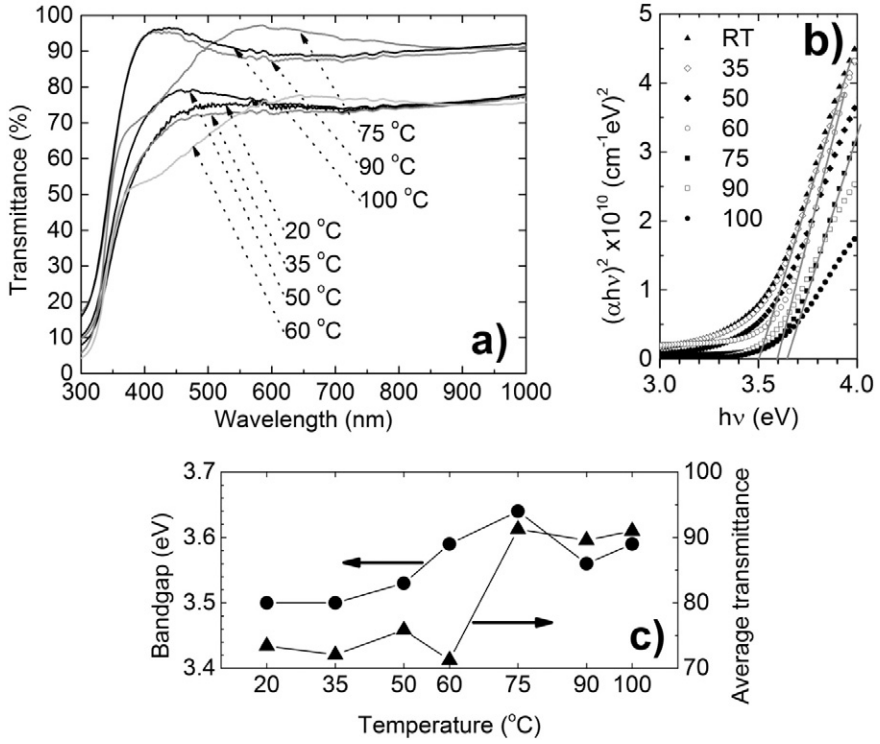


**Fig. 3.** a) Transmittance, b) $(\alpha h\nu)^2$ vs $h\nu$ plots and c) extracted bandgap and average transmittance of the AZO films deposited at different substrate temperatures.

The Hall Effect measurement results are plotted in Fig. 4. All the AZO films produced Hall voltages indicating an n-type behavior. The lowest resistivity of $8.8 \times 10^{-4}$ Ω-cm was obtained at 75 °C. For this temperature, the mobility reached its highest value of 20 $cm^2$/V-s. From the carrier concentration values ($>1 \times 10^{20}$ $cm^{-3}$), we can conclude that all the AZO films are degenerate. The electrical resistivity varied from $8.8 \times 10^{-4}$ (75 °C) to $3.1 \times 10^{-3}$ Ω-cm (90 °C), while for all the remaining samples the resistivity was in the order of $1.3 \times 10^{-3}$ Ω-cm. So there is not a strong variation of the resistivity with the substrate temperature in this range. The lowest mobility and the highest carrier concentration were reached when the substrate temperature is equal to 60 °C which confirms that in our system at this temperature there is a transition not only in the structural and optical, but also on the electrical properties.

In order to evaluate the transparent conductive properties of the AZO films, a figure of merit (FOM) was examined. Since a high conductivity and at the same time a high optical transmittance is desired, the FOM can be defined as [24]:

$$FOM = -\frac{1}{\rho \ln T} \tag{2}$$

where $T$ and $\rho$ are the average transmittance and resistivity, respectively. As shown in Fig. 5, the value of the FOM, for the prepared films, achieves a maximum value of ~12,500 for the substrate temperature of 75 °C and remains almost constant at ~3000 for other temperatures. The FOM value for substrates at 75 °C is comparable and even higher to that obtained for thicker films (>200 nm), as reported in the literature [19,25].

The polycrystalline nature of the AZO films, produced by the coexistence of the crystallites with orientation in the (002) and (103) planes at a substrate temperature higher than 60 °C, improves the average transmittance while the resistivity, mobility and carrier concentration remains almost constant (orders of magnitude). The small change in the electrical properties is correlated to the small change in the grain sizes. The AZO film deposited at 75 °C was chosen as the optimized film for the fabrication of TFTs, as described below.

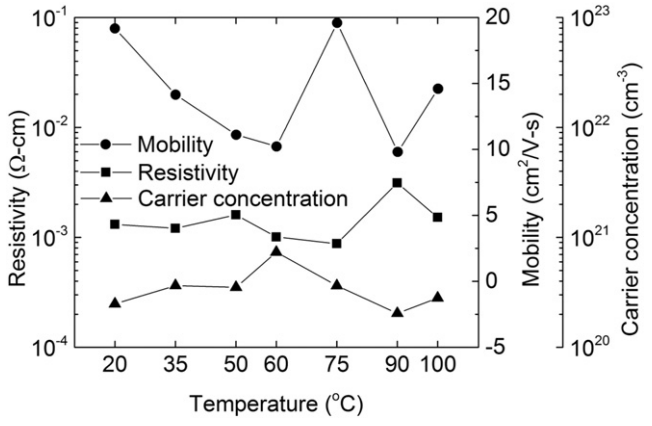


**Fig. 4.** Hall effect measurements of the AZO films deposited at different substrate temperatures.

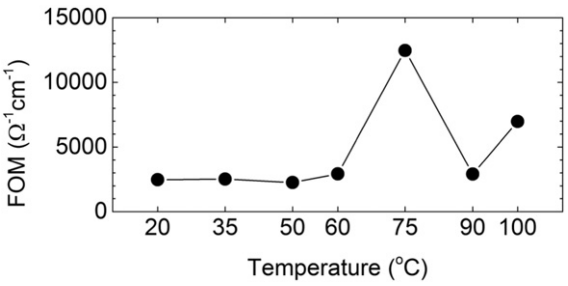


**Fig. 5.** The FOM of AZO films as a function of the substrate temperature.

### 3.2. Device characterization

The device structure and the fabricated device are shown in Fig. 6a and Fig. 6b, respectively. The AZO films deposited at 75 °C were used as ohmic contacts to ZnO. Both ZnO and AZO films were deposited in the same sputtering chamber. Further improvement of the device structure showed in Fig. 6a will consist in using AZO as the gate metal and developing a dielectric by sputtering for a full fabrication process by a confocal sputtering. During the fabrication process, the AZO films are easily patterned by wet etching with a solution of HCl:$H_2O$ 1:500 for 1 min.

In Fig. 7a, the representative drain current ($I_{DS}$) versus gate voltage ($V_{GS}$) transfer characteristic is plotted. The values for the field effect mobility ($\mu_{FET}$) and threshold voltage ($V_T$), were calculated from the slope and extrapolation of the $I_{DS}^{1/2}$ versus $V_{GS}$ curve in saturation as elsewhere [16]. The extracted $\mu_{FET}$ and $V_T$ were 21 $cm^2$/V-s and 7 V, respectively, while the $I_{on}/I_{off}$ ratio was $10^9$ for the three different channel lengths. The gate current ($I_{GS}$) remained constant at $1 \times 10^{-11}$ A for all the devices. The representative $I_{DS}$ versus drain voltage ($V_{DS}$) output characteristic is shown in Fig. 7b. It is observed that the channel can be completely closed at 0 V. The contact resistance at the AZO/ZnO interface should be low enough to produce a high output current (>200 μA) and $I_{on}/I_{off}$ ratio. Since the resultant mobility and threshold voltage depends upon the interface quality between the semiconductor and the gate dielectric, further optimization needs to be done for the semiconductor ZnO layer. This optimization is being carried out in order to reduce the threshold voltage (near 0 V) while maintaining the high mobility (>10 $cm^2$/V-s). By fabricating TFTs with different channel lengths and similar width lengths, it is possible to extract the contact resistance at the AZO/ZnO interface by the transfer length method. The total resistance ($R_T$) is composed by the sum of two times the contact resistance ($R_c$) and the semiconductor sheet resistance ($R_{sh}$) as depicted in the inset of Fig. 8. The total resistance is obtained for each channel length by fitting the linear portion of the $I_{DS}$–$V_{GS}$ curve ($V_{GS} > V_T$) when the $V_{DS}$ is equal to 1 V as found in the literature [26]. In this method, the total resistance is also known as the ON-resistance because the channel is already created. Then, the total resistance is plotted versus the channel length as shown in Fig. 8. A linear fit is performed to these three points and then the $R_c$, $R_{sh}$, resistivity of the ZnO ($\rho_{ZnO}$) and the specific contact resistance ($\rho_c$) are obtained as described in [27] and their values are shown in Fig. 8. The obtained $\rho_c$ equals 0.06 Ω-$cm^2$ which is high when compared to reported values of the order of $10^{-4}$ Ω-$cm^2$ (without annealing) and $10^{-6}$ Ω-$cm^2$ after performing high temperature annealing (>600 °C) using ITO contacts [28,29]. However, to the best of our knowledge, our results correspond to the first report of the ZnO/AZO specific contact resistance obtained with a maximum processing temperature of 100 °C. Few efforts have been done in determining the quality of ohmic contacts for devices processed at these low temperatures, especially for flexible and transparent electronic devices. Further studies need to be done for analyzing the impact of the AZO film thickness and deposition parameters in the performance of the ZnO-based TFTs and the reduction of the specific contact resistance.

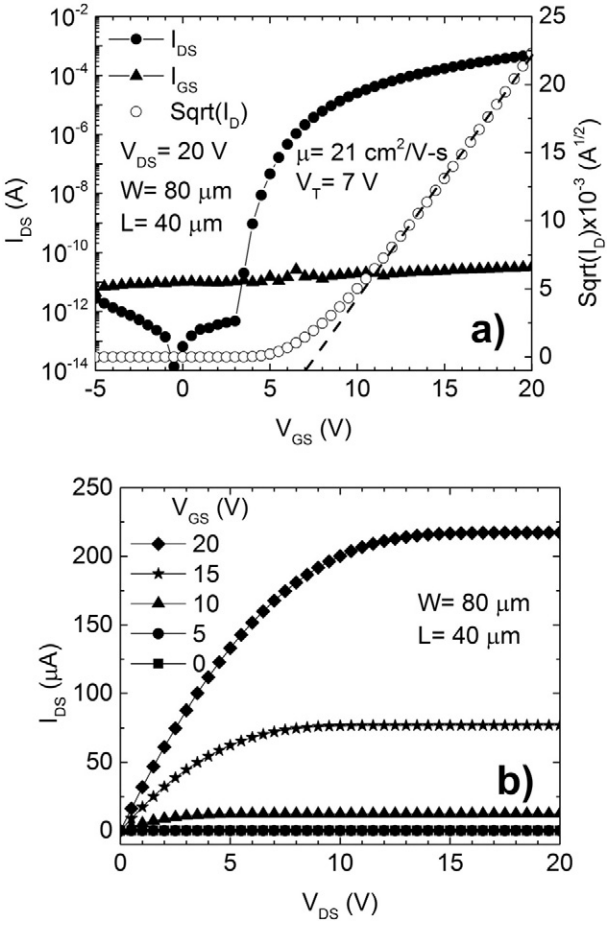


**Fig. 7.** a) $I_{DS}$–$V_{GS}$ and b) $I_{DS}$–$V_{DS}$ plots of the fabricated devices ($W = 80$ μm and $L = 40$ μm).

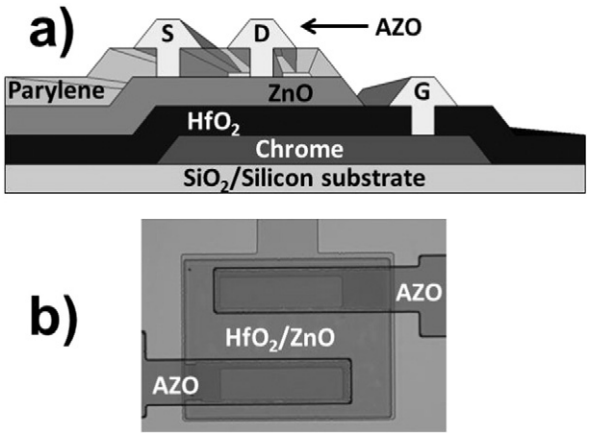


**Fig. 6.** a) Schematics of the fabricated TFTs. b) Optical microscope image of the completed device ($W = 80$ μm and $L = 40$ μm).

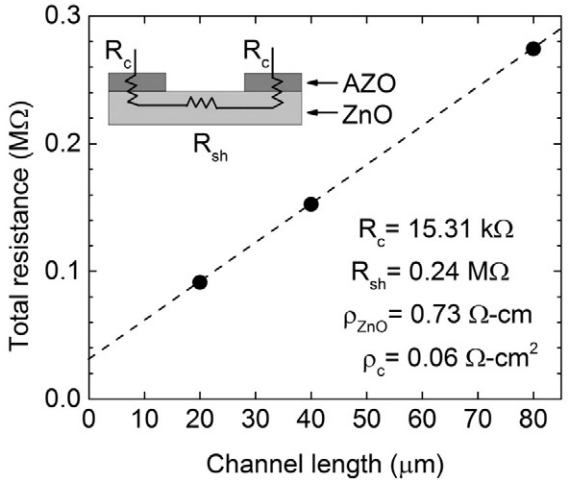


**Fig. 8.** Transfer length method used for estimating $R_c$ and $\rho_c$. The inset shows the composition of the total resistance.

## 4. Conclusion

The impact of the substrate temperature on the electrical, optical and structural properties of AZO films deposited by confocal sputtering was investigated. It was found that the substrate temperature plays an important role by producing polycrystalline films with enhanced transparency and bandgap. Polycrystalline AZO films, with preferential crystallite planes in the (002) and (103) orientations of the zincblende (hexagonal) structure, are obtained at substrate temperatures higher than 60 °C which improve the optical and electrical properties of the films. We have shown that the optimum substrate temperature is 75 °C. At this temperature, the FOM used for this work, the resistivity and the average transmittance reached values of $1.3 \times 10^4\ \Omega^{-1}$-cm$^{-1}$, $8.8 \times 10^{-4}\ \Omega$-cm and 91%, respectively. ZnO-based TFTs were uniformly fabricated with the AZO films working as source-drain electrodes over a 4 in. wafer area. High mobility devices (~20 cm$^2$/V-s) were obtained with a specific contact resistance of 0.06 Ω-cm$^2$. The low temperature process (<100 °C) and the use of transparent films make the ZnO-based TFTs fabricated here suitable for flexible and transparent electronics. It was also demonstrated that the use of confocal sputtering can be further extended for large area fabrication of devices were all the films (semiconductor, electrodes and dielectrics) are deposited in one single chamber with improved usage of the targets in consideration with the substrate size.

## Acknowledgments

This work was partially supported by the CONACYT-Mexico under grants CB-2010/158281 and CB-2014/240103.

## References

[1] H. Liu, V. Avrutin, N. Izyumskaya, Ü. Özgür, H. Morkoç, Superlattice. Microst. 48 (2010) 458–484.
[2] Ü. Özgür, Y.I. Alivov, C. Liu, A. Teke, M.A. Reshchikov, S. Dogan, V. Avrutin, S.-J. Cho, H. Morkoç, J. Appl. Phys. 98 (041301) (2005).
[3] G.B. Murdoch, S. Hinds, E.H. Sargent, S.W. Tsang, L. Mordoukhovski, Z.H. Lu, Appl. Phys. Lett. 94 (2009) 213301.
[4] X. Zou, G. Fang, J. Wan, N. Liu, H. Long, H. Wang, X. Zhao, Semicond. Sci. Technol. 26 (2011) 055003.
[5] D.-J. Yun, S.-W. Rhee, Thin Solid Films 517 (2009) 4644–4649.
[6] W. Beyer, J. Hüpkes, H. Stiebig, Thin Solid Films 516 (2007) 147–154.
[7] W. Yang, Z. Liu, D.-L. Peng, F. Zhang, H. Huang, Y. Xie, Z. Wu, Appl. Surf. Sci. 255 (2009) 5669–5673.
[8] Y.H. Kim, K.S. Lee, T.S. Lee, B. Cheong, T.-Y. Seong, W.M. Kim, Appl. Surf. Sci. 255 (2009) 7251–7256.
[9] M. Berginski, J. Hüpkes, M. Schulte, G. Schöpe, H. Stiebig, B. Rech, M. Wutting, J. Appl. Phys. 101 (2007) 074903.
[10] K.-W. Sun, W.-C. Zhou, S.-S. Huang, X.-F. Tang, J. Inorg. Mater. 27 (10) (2012) 1112–1116.
[11] Z. Zhang, C. Bao, S. Ma, L. Zhang, S. Hou, J. Aust. Ceram. Soc. 48 (2) (2012) 214–222.
[12] E. Miorin, F. Montagner, S. Battiston, S. Fiameni, M. Fabrizio, J. Nanosci. Nanotechnol. 10 (2010) 1–5.
[13] S. Fernandez, A. Martinez-Steele, J.J. Gandia, F.B. Naranjo, Thin Solid Films 517 (2009) 3152–3156.
[14] S. Teehan, H. Efstathiadis, P. Haldar, J. Alloy, Compound 509 (2011) 1094–1098.
[15] S. Jay Chey, W. Liu, M. Yuan, D.B. Mitzi, 34th IEEE Photovoltaic Specialists Conference, Philadelphia, PA, 2009.
[16] G. Gutierrez-Heredia, I. Mejia, M.E. Rivas-Aguilar, N. Hernandez-Como, V.H. Martinez-Landeros, F.S. Aguirre-Tostado, M.A. Quevedo-Lopez, Thin Solid Films 545 (2013) 458–461.
[17] M. Fox, Optical properties of solids, 1st edn Oxford University Press, New York, 2001 58–60.
[18] S.S. Shinde, S. Prakash, R.S. Patil, R.S. Gaikwad, B.N.P. Mane, K.Y. Rajpure, J. Alloys Compd. 503 (2010) 416–421.
[19] B.L. Zhu, J. Wang, S.J. Wu, D.W. Zeng, C.S. Xie, Phys. Status Solidi A 209 (2012) 1251–1258.
[20] Q. Hou, F. Meng, J. Sun, Nanoscale Res. Lett. 8 (2013) 144.
[21] C.-H. Huang, H.-L. Cheng, W.-E. Chang, M.-S. Wong, J. Electrochem. Soc. 158 (2011) H510–H515.
[22] X.-Y. Gao, Q.-G. Lin, H.-L. Feng, Y.-F. Liu, J.-X. Lu, Thin Solid Films 517 (2009) 4684–4688.
[23] I. Mejia, A.L. Salas-Villasenor, A. Avendano-Bolivar, J. Horvath, H. Stiegler, B.E. Gnade, M.A. Quevedo-Lopez, IEEE Electr. Device L. 32 (2011) 1086–1088.
[24] R.E.I. Schropp, A. Madan, J. Appl. Phys. 66 (1989) 2027–2031.
[25] S. Fernandez, F.B. Naranjo, S. Valdueza-Felip, O. de Abril, Phys. Status Solidi A 207 (2010) 1717–1721.
[26] D. Boudinet, G. Le Blevennec, C. Serbutoviez, J.-M. Verilhac, H. Yan, G. Horowitz, J. Appl. Phys. 105 (2009) 084510.
[27] D.K. Schroder, Semiconductor Material and Device Characterization, John Wiley & Sons, Second edition, 1998 143–151.
[28] C.-C. Ho, L.-W. Lai, C.-T. Lee, K.-C. Yang, B.-T. Lai, D.-S. Liu, J. Phys. D. Appl. Phys. 46 (2013) 315102.
[29] Y.-Z. Chiou, K.-W. Lin, J. Electrochem. Soc. 153 (2006) G141–G142.